Guided modes supported by plasmonic films with a periodic arrangement of subwavelength slits

Peter B. Catrysse,[a] Georgios Veronis, Hocheol Shin, Jung-Tsung Shen, and Shanhui Fan
Edward L. Ginzton Laboratory, Stanford University, Stanford, California 94305-4088

(Received 14 April 2005; accepted 16 November 2005; published online 17 January 2006)

We calculate the guided band diagram of a metallic film with a one-dimensional periodic arrangement of cut-through subwavelength slits. We find that this system supports two distinct types of guided modes propagating in a direction perpendicular to the slits when the metal obeys a plasmonic dispersion model. The first type is a well-known surface mode. The second type results from the presence of a subwavelength electromagnetic resonance inside the slits and closely resembles waveguide modes in a dielectric slab. We refer to them as effective dielectric slab modes. We show how the behavior of both modes is affected by film thickness and surface properties. © *2006 American Institute of Physics*. [DOI: 10.1063/1.2164905]

Recently, there has been strong interest in the optical properties of metallic films with a one-dimensional periodic arrangement of cut-through subwavelength slits.[1–5] Most works have focused on the transmission properties. For transmission, the phase space of interest is located above the light line $\omega=ck_x$ in the (k_x,ω) plane, where k_x is the x component of the wave vector (perpendicular to the slits; Fig. 1), ω is the frequency, and c is the speed of light. In this letter, we focus on guided modes that lie below the light line. This region has remained unexplored. Understanding the behavior of guided modes is potentially important for integrated optics applications. Moreover, it has been pointed out quite recently that the behavior of guided modes is intimately related to the use of such a system as a metamaterial with unusual dielectric properties.[6,7] In this context, it is important to examine the properties of guided modes with more realistic material models for the metal. Here, we find in the long-wavelength regime that the system shown in the inset in Fig. 1 supports two distinct types of transverse-magnetic (TM) guided modes propagating in a direction perpendicular to the slits when the metal is described by a plasmonic model [TM modes have magnetic fields parallel to the slits (H_z)]. The first type is a well-known *surface mode*. This mode is confined to the front and back metal-dielectric interfaces of the film. The second type originates from a subwavelength electromagnetic state supported by the slits. In slits, regardless of how narrow they are, there always exists a propagating state. In the transmission regime, this state enables enhanced transmission.[2–4] In the guided regime, this state gives rise to guided modes, which closely resemble wave guide modes in a dielectric slab. We refer to them as *effective dielectric slab modes*.

We calculate the dispersion relations of the guided modes supported by the metallic film using a finite-difference frequency-domain method. Specifically, we solve the wave equation for H_z (E_z) in the case of TM [transverse-electric (TE)] polarization.[8,9] The computational domain consists of a single period of the structure. We use the following boundary condition at the left and right boundaries[10]

$$\phi(x+d)=\exp(ik_x d)\,\phi(x), \tag{1}$$

where d is the periodicity of the structure and $\phi=H_z$ (E_z) for TM (TE) polarization. Perfectly matched layer (PML) absorbing boundary conditions are used at the top and bottom boundaries.[11] We excite a point source and the resulting frequency spectrum at detector points is composed of a discrete set of peaks, where each peak corresponds to an eigenfrequency.

We describe the optical properties of the metal using a Drude free-electron model:

$$\varepsilon_2(\omega)=1-\frac{\omega_p^2}{\omega(\omega-i\omega_\tau)}, \tag{2}$$

where ω_p is the plasma frequency and ω_τ is the collision frequency. This dielectric function takes into account the contribution of free electrons only. We refer to it as the *plasmonic model*. Despite its apparent simplicity, the plasmonic model has been the source of valuable insights into the general behavior of real metals. In the guided band diagram calculations presented here, we assume a lossless plasmonic model in which we neglect absorption by setting the collision

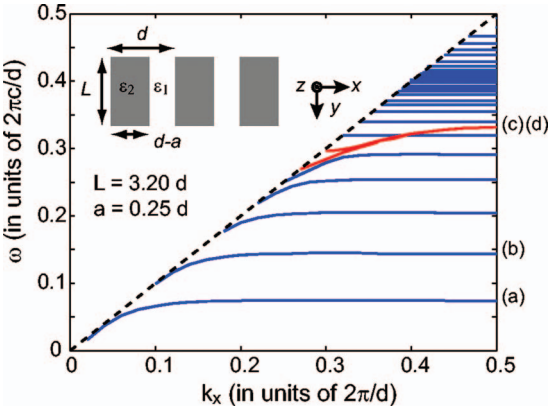

FIG. 1. (Color) Guided-mode band diagram for TM polarization (first Brillouin zone) when $L=256$ nm, $d=80$ nm, $a=20$ nm. Shown are two degenerate surface modes (red curves) and a series of effective dielectric slab modes (blue curves). The dashed line is the light line in vacuum. Inset shows the schematic of a metallic film with periodic slits: a is the slit width, d is the periodicity, and L is the film thickness. The gray regions indicate metal (ε_2) and the white regions represent vacuum $(\varepsilon_1=1)$.

[a]Electronic mail: pcatryss@stanford.edu

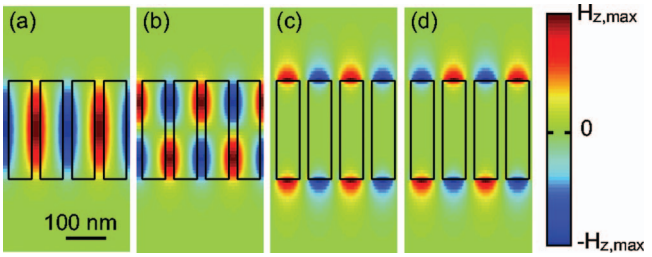

FIG. 2. (Color) H_z-field distributions for the two types of guided modes supported by the geometry shown in Fig. 1. Distributions are shown for $k_x=0.50$ in units of $2\pi/d$. Frequencies ω are given in units of $2\pi c/d$. (a) Fundamental effective dielectric slab mode at $\omega=0.074$, (b) next-higher-order effective dielectric slab mode at $\omega=0.144$, and (c) and (d) surface modes at $\omega=0.332$. Red and blue correspond to large positive and negative field values, respectively, and green represents zero field.

frequency to zero, $\omega_\tau=0$. It was found from previous band diagram calculations of metallic photonic crystals, in which a plasmonic model was used, that the real part of the band structure is hardly affected by absorption for realistic amounts of absorption.[12] We use $\omega_p=1.368\,84\times10^{16}$ rad/s, which is representative of metals (e.g., silver). Without loss of generality, we also assume hereafter vacuum ($\varepsilon_1=1$) for the ambient dielectric environment and the slit regions.

Figure 1 shows the band diagram (in the first Brillouin zone) for the guided modes in TM polarization (H_z). The metallic film has a thickness $L=256$ nm. The slits have periodicity $d=80$ nm and width $a=20$ nm. The guided band diagram features two distinct types of modes: Two surface modes (red curves) and a series of effective dielectric slab modes (blue curves). The surface modes are confined to the top and bottom metal-vacuum interfaces, respectively. They are degenerate and have the characteristics of surface plasmon modes on a flat surface. At low frequencies ω, the surface modes asymptotically approach the light line in the ambient environment. The band approaches $\omega=0.332\cdot2\pi c/d$ at the Brillouin zone edge. At large values of the propagation constant k_x, in an extended Brillouin zone representation, we expect the frequency of the surface modes to approach the surface plasmon frequency $\omega_p/\sqrt{2}$ of the metal-vacuum interface. However, in this system, it becomes difficult to distinguish between the surface modes and the effective dielectric slab modes above $\omega=0.332\cdot2\pi c/d$.

The slits in the plasmonic film, regardless of how narrow they are, always support a propagating state. This state gives rise to a series of effective dielectric slab modes. These modes derive their name from the fact that a similar perfect electric conductor (PEC) system has been shown to be equivalent to a dielectric slab with an effective refractive index.[6] At low frequencies ω, they follow the light line in a vacuum. At large k_x, the frequencies approach a series of limiting values, which depend on the order of the mode. While the limiting frequency values are co-determined by geometrical and material parameters, the large-k_x behavior of these modes is quite similar to that of the effective dielectric slab modes found in a PEC system.[6] In the PEC case, the limiting values at large k_x are equally spaced and they are related to the Fabry–Perot resonance condition. Here, they become increasingly closer to each other as frequency increases.

Figure 2 depicts the field distributions of the modes presented in Fig. 1 for $k_x=0.50$ (in units of $2\pi/d$). All modes

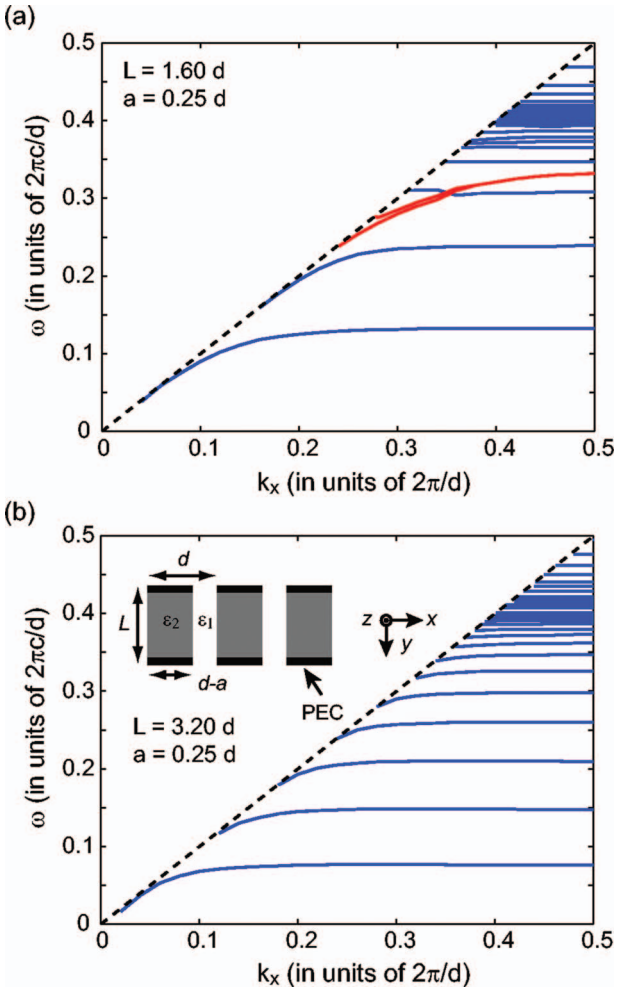

FIG. 3. (Color) Effects of film thickness and surface properties on the guided-mode band diagram for TM polarization. Shown are two degenerate surface modes (red curves) and a series of effective dielectric slab modes (blue curves). The dashed line is the light line in vacuum. (a) Reduction in film thickness ($L=128$ nm, $d=80$ nm, $a=20$ nm) and (b) perfect electric conductor (PEC) coating on plasmonic film. Inset shows the schematic of the metal film with periodic slits. The gray regions indicate metal (ε_2) coated with a thin PEC film (black) and the white regions represent vacuum ($\varepsilon_1=1$).

propagate in the x direction. Shown are the H_z-field distribution of: The fundamental effective dielectric slab mode [Fig. 2(a)], the next-higher-order effective dielectric slab mode [Fig. 2(b)], and both degenerate surface modes [Figs. 2(c) and 2(d)]. The surface modes are confined to the lower and upper metal-vacuum interface of the film, respectively. Their field decays rapidly as the distance from the interface increases, as expected. The effective dielectric slab modes, on the other hand, have their maximum within the slits of the system and thus indeed resemble the guided modes in a dielectric slab.

Since the system supports two distinct types of guided modes, each with a clear signature for large slab thickness, it is to be expected that these modes will also behave differently when the system parameters are modified. Through the careful choice of the geometrical and surface properties, it is possible to control the presence or absence of plasmonic modes and to change their dispersion properties. Figure 3(a) shows the dispersion relations when the film thickness L is reduced by a factor of 2 ($L=128$ nm, $d=80$ nm, $a=20$ nm). For the effective dielectric slab modes, this reduction has a

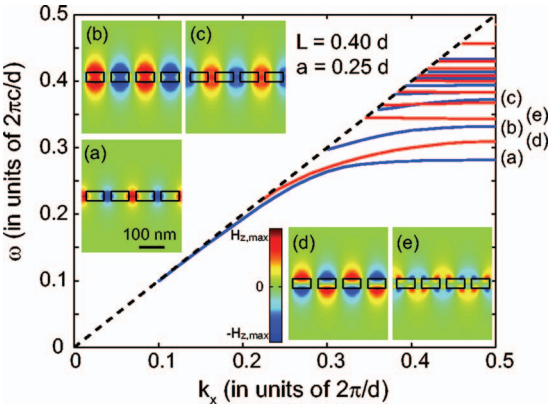

FIG. 4. (Color) Guided-mode band diagram for TM polarization (first Brillouin zone) when $L=32$ nm, $d=80$ nm, $a=20$ nm. Shown are a series of odd (red curves) and even (blue curves) modes. The dashed line is the light line in vacuum. Insets show the field distributions for $k_x=0.50$. (a) H_z-field distribution for the fundamental effective dielectric slab mode at $\omega=0.282$; (b) and (c) H_z-field distribution of the symmetric (even) coupled modes at $\omega=0.332$ and $\omega=0.372$, respectively; and (d) and (e) H_z-field distribution of antisymmetric (odd) coupled modes at $\omega=0.309$ and $\omega=0.343$, respectively. Red and blue correspond to large positive and negative field values, respectively, and green represents zero field.

profound impact on the behavior at large k_x values: The series of limiting frequency values shift up in a manner which is inversely proportional to L. The thickness of the film affects the Fabry–Perot resonance condition of the electromagnetic state in the slits on which the effective dielectric slab modes rely for their existence. The surface mode, on the other hand, is almost unaffected by the change in thickness as long as the thickness is large compared to the decay length of the mode inside the slits. The surface modes can be removed if the top and bottom interfaces of the plasmonic film are coated with a thin PEC layer [Fig. 3(b)], since the PEC-vacuum interface does not support a surface mode. The effective dielectric slab modes, on the other hand, remain almost unchanged.

It is known that surface modes on a periodic structure exhibit a band gap due to periodic scattering.[13,14] For large film thickness L, the presence of the effective dielectric slab modes obfuscates the band gap. To clearly see the gap behavior, one needs to significantly reduce L. For example, Fig. 4 presents the dispersion relations of the plasmonic modes for a film thickness of 32 nm. This alters the dispersion relation of the effective dielectric slab modes by pushing up the limiting values (flat bands) toward higher frequencies. The insets depict the H_z-field profiles for the different modes. The field profile plot of the fundamental effective dielectric slab mode, shown in the inset of Fig. 4(a), is not much modified from the profile of the same mode in a thicker film [see Fig. 2(a)]. Hence, this mode is still clearly identifiable as an effective dielectric slab mode. For the other modes, there are two consequences to the dispersion relation. First, there is a splitting of the degenerate single-interface modes into two coupled surface modes.[15] These modes are neither pure surface modes nor effective dielectric slab modes anymore. The coupled modes can be easily distinguished based on the symmetry of the H_z-field profiles with respect to the xz plane through the middle of the film and are referred to as symmetric (insets b and c) and antisymmetric (insets d and e) modes. Second, a band gap is formed. Below and above the band gap, the modes have their maximum or minimum either at the metal (insets b and d) or at the slit (insets c and e) as a result of the folding at the edge of the first Brillouin zone. These modes delineate the lower and upper limits of a small band gap, which can be estimated at $\Delta\omega_{bc}=0.040$ and $\Delta\omega_{de}=0.034$ in units of $2\pi c/d$. Finally, under certain conditions, the bands of these two types of modes can cross and mode coupling occurs. For example, in Fig. 1 this occurs for $k_x=0.39$ and $\omega=0.320$. Under these circumstances, a small frequency variation can give rise to a large change in the field distribution from slit confined to surface confined.

As final remarks, using tabulated data for the dielectric function of silver,[16] we have also analyzed the guided band diagram of this system. For real metal parameters, the main conclusion of the letter, i.e., the existence of two types of guided modes, remain valid. A similar analysis for TE polarization, with the electric field parallel to the slits (E_z), revealed that the system does not support any guided modes propagating in the x direction in this polarization. This finding agrees with the results obtained for a PEC system.[6]

This work was supported in part by National Science Foundation Grant No. ECS-0134607 and by Air Force Office of Scientific Research Grant No. FA9550-04-1-0437.

[1] F. J. Garcia-Vidal and L. Martin-Moreno, Phys. Rev. B **66**, 155412 (2002).
[2] J. A. Porto, F. J. Garcia-Vidal, and J. B. Pendry, Phys. Rev. Lett. **83**, 2845 (1999).
[3] J. T. Shen and P. M. Platzman, Phys. Rev. B **70**, 035101 (2004).
[4] Y. Takakura, Phys. Rev. Lett. **86**, 5601 (2001).
[5] P. N. Stavrinou and L. Solymar, Opt. Commun. **206**, 217 (2002).
[6] J.-T. Shen, P. B. Catrysse, and S. H. Fan, Phys. Rev. Lett. **94**, 197401 (2005).
[7] F. J. Garcia-Vidal, L. Martin-Moreno, and J. B. Pendry, J. Opt. A, Pure Appl. Opt. **7**, S97 (2005).
[8] G. Veronis, R. W. Dutton, and S. H. Fan, Opt. Lett. **29**, 2288 (2004).
[9] S. D. Wu and E. N. Glytsis, J. Opt. Soc. Am. A **19**, 2018 (2002).
[10] S. H. Fan, P. R. Villeneuve, and J. D. Joannopoulos, J. Phys.: Condens. Matter **54**, 11245 (1996).
[11] J.-M. Jin, *The Finite Element Method in Electromagnetics*, 2nd ed. (Wiley, New York, 2002).
[12] H. van der Lem, A. Tip, and A. Moroz, J. Opt. Soc. Am. A **20**, 1334 (2003).
[13] S. I. Bozhevolnyi, J. Erland, K. Leosson, P. M. W. Skovgaard, and J. M. Hvam, Phys. Rev. Lett. **86**, 3008 (2001).
[14] S. C. Kitson, W. L. Barnes, and J. R. Sambles, Phys. Rev. Lett. **77**, 2670 (1996).
[15] E. N. Economou, Phys. Rev. **182**, 539 (1969).
[16] E. D. Palik, *Handbook of Optical Constants of Solids* (Academic, Orlando, 1985).